Reprinted from

THE PHYSICS OF FLUIDS VOLUME 9, NUMBER 5 MAY 1966

Microinstability and Shear Stabilization of a Low-β, Rotating, Resistive Plasma

FRANCIS F. CHEN
Plasma Physics Laboratory, Princeton University, Princeton, New Jersey
(Received 12 October 1965)

A magnetoplasma in a radial electric field E_r suffers from a gravitational instability driven by the centrifugal force. By using only fluid equations, the theory of Rosenbluth, Krall, and Rostoker was extended to finite $k_\parallel$ and finite resistivity. The theory of resistive drift modes in cylindrical geometry is included as the limit $E_r \to 0$. The shear stabilization was computed, and it was found that the drift modes are not localized by shear unless ion Landau damping is taken into account. A stabilization criterion was obtained which is much more severe than those found previously and which is almost impossible to fulfill experimentally. However, it is the modes with short radial wavelength which are most difficult to stabilize, and these may not be harmful to plasma confinement. The role of the Coriolis force and the importance of these instabilities to experiments in cesium plasmas, stellarators, rotating plasmas, and beam-plasma discharges are also pointed out. This theory is particularly germane to cesium plasmas, in which it is shown that E_r cannot be ignored.

I. INTRODUCTION

When a fully ionized cylindrical plasma column is made to rotate under a radial electric field E_r, the centrifugal force resulting from the rotation can produce a Rayleigh–Taylor "gravitational" instability, which tends to destroy density gradients in the plasma and, hence, cause the column to spread out radially. This centrifugal instability was first treated by Rosenbluth, Krall, and Rostoker[1] and has been observed experimentally in high-β plasmas by Kolb *et al.*[2,3] Our purpose here is fivefold: (1) to point out the importance of this instability in certain low-β experiments; (2) to show that the results of Ref. 1 can be obtained from fluid equations without using kinetic theory; (3) to extend the results of Ref. 1 to larger values of E_r, to finite $k_\parallel$ and finite resistivity η, and to arbitrary T_i/T_e; (4) to point out the role of the Coriolis force, and (5) to compute the shear stabilization.

The complexity of the problem stems from the fact that the effects of finite Larmor radius r_L, cylindrical geometry, and radial boundaries must all be taken into account. We use a fluid model, taking finite r_L into account by means of the ion viscosity tensor π_i in cylindrical coordinates. A result of this approach is that the reason for a puzzling asymmetry in the result of Ref. 1 becomes clear. Rosenbluth *et al.*[1] found that the instability sets in at smaller values of the rotation velocity $r\Omega_0$ for $\Omega_0 > 0$ than for $\Omega_0 < 0$. The reason is that the Coriolis force, which depends on the sign of Ω_0 whereas the centrifugal force does not, produces a drift with a stabilizing effect if $\Omega_0 < 0$.

The centrifugal instability is particularly interesting because it is the only example of a gravitational instability in a cylindrically symmetric situation. If, for instance, the "gravitational" force were due to a curvature in the field lines, one would have to treat the problem in a torus rather than in the simpler infinite cylinder. The centrifugal instability also provides a mechanism for the transport of plasma across the magnetic field when only one species is initially unstable. For instance, high-frequency instabilities can cause the loss of electrons but cannot directly affect the ions. What happens then is that an electric field builds up, causing the plasma to rotate, and the ions are lost by the resulting low-frequency instability.

II. FUNDAMENTAL EQUATIONS

Following our previous treatment[4] of resistive drift waves in very low-β plasmas, we write the equations of motion and continuity of the ion and electron fluids as follows:

$$\frac{\partial \mathbf{v}}{\partial \tau} + \mathbf{v}\cdot\nabla\mathbf{v} = -\nabla\chi - \lambda\frac{\nabla n}{n} + \mathbf{v}\times\hat{\mathbf{z}} - \lambda\left(\nabla\cdot\mathbf{\Pi} + \mathbf{\Pi}\cdot\frac{\nabla n}{n}\right) + \epsilon(\mathbf{v}_e - \mathbf{v}), \quad (1)$$

$$0 = \nabla\chi - (\nabla n/n) - \mathbf{v}_e\times\hat{\mathbf{z}} + \epsilon(\mathbf{v} - \mathbf{v}_e), \quad (2)$$

$$-\partial n/\partial\tau = \nabla\cdot(n\mathbf{v}) = \nabla\cdot(n\mathbf{v}_e), \quad (3)$$

where $\mathbf{v} = \mathbf{v}_i/v_s$, $\mathbf{v}_e = \mathbf{v}_e/v_s$, $v_s^2 = KT_e/m_i$, $\tau = \omega_c t$, $\omega_c = eB/m_i$, $\mathbf{B} = B\hat{\mathbf{z}}$, $\lambda = T_i/T_e$, $\chi = e\phi/KT_e$, $\epsilon = ne\eta/B$, $\mathbf{\Pi} = \pi_i/nKT_i$, and ∇ is in units of $a^{-1} \equiv$

[1] M. N. Rosenbluth, N. A. Krall, and N. Rostoker, Nucl. Fusion Suppl. Pt. 1, 143 (1962).
[2] N. Rostoker and A. C. Kolb, Phys. Rev. 124, 965 (1961).
[3] A. C. Kolb, P. C. Thonemann, and E. Hintz, Phys. Fluids 8, 1005 (1965); E. Hintz and A. C. Kolb, *ibid.* 8, 1347 (1965).
[4] F. F. Chen, Phys. Fluids 8, 1323 (1965).

ω_e/v_s. These equations are valid for quasi neutral, isothermal plasmas with $\beta \equiv (8\pi nKT/c^2B^2) \ll (m_e/m_i)$ and $(m_e/m_i) \to 0$. Furthermore, in the perturbed equations we shall neglect v_z and $\eta_\perp$, as is permissible[4] for drift waves in the absence of classical diffusion. Then finite-r_L effects occur only in Eq. (1), and finite-η effects only in the z component of Eq. (2).

In cylindrical coordinates (r, θ, z) (normalized to the length a), the viscosity tensor given in Ref. 4 takes the form

$$\begin{aligned}
-\Pi_{rr} &= \frac{1}{3}\alpha\left(v_{r,r} + \frac{1}{r}v_r + \frac{1}{r}v_{\theta,\theta} - 2v_{z,z}\right) + \frac{1}{2}\left(v_{\theta,r} + \frac{1}{r}v_{r,\theta} - \frac{1}{r}v_\theta\right), \\
-\Pi_{\theta\theta} &= \frac{1}{3}\alpha\left(v_{r,r} + \frac{1}{r}v_r + \frac{1}{r}v_{\theta,\theta} - 2v_{z,z}\right) - \frac{1}{2}\left(v_{\theta,r} + \frac{1}{r}v_{r,\theta} - \frac{1}{r}v_\theta\right), \\
-\Pi_{r\theta} &= \frac{1}{2}\left(-v_{r,r} + \frac{1}{r}v_r + \frac{1}{r}v_{\theta,\theta}\right) + \frac{1}{4\alpha}\left(v_{\theta,r} + \frac{1}{r}v_{r,\theta} - \frac{1}{r}v_\theta\right) - \tfrac{1}{3}v_{z,z} = -\Pi_{\theta r}, \\
-\Pi_{zz} &= \frac{2}{3}\alpha\left(2v_{z,z} - v_{r,r} + \frac{1}{r}v_r + \frac{1}{r}v_{\theta,\theta}\right),
\end{aligned} \tag{4}$$

where the comma denotes differentiation and $\alpha \equiv \omega_e\tau_{ii}$. The ion–ion collision frequency τ_{ii} is proportional to n^{-1}, and therefore, α is a function of position. The components Π_{rz} and $\Pi_{\theta z}$ contain only terms in v_z or $\partial/\partial z$ without the large factor α and may be neglected straightway with the drift-wave approximation $k_\parallel \ll k_\perp$, and hence, $v_z \ll v_\perp$.

For the equilibrium state we imagine an infinitely long cylindrical plasma in a uniform $\mathbf{B}$ with $\partial/\partial\theta = \partial/\partial z = \partial/\partial\tau = v_z = v_{ez} = 0$; a radial electric field E_r causes the plasma to rotate about its axis. We neglect $\mathbf{\Pi}_0$ for the time being and solve Eqs. (1) and (2) for $\mathbf{v}_0$ and $\mathbf{v}_{e0}$, keeping only lowest order in ϵ, which is generally less than 10^{-4}. The centrifugal and Coriolis forces are contained in the term $\mathbf{v}\cdot\nabla\mathbf{v}$ in cylindrical coordinates. We obtain

$$v_{\theta 0}(1 + r^{-1}v_{\theta 0}) = \lambda\delta - \mathcal{E}_r; \quad v_{e\theta 0} = -(\delta + \mathcal{E}_r), \tag{5}$$

$$v_{r0} = -(1 + 2r^{-1}v_{\theta 0})^{-1}\bar{\lambda}\epsilon\delta, \quad v_{er0} = -\bar{\lambda}\epsilon\delta, \tag{6}$$

where $\delta \equiv n_0^{-1}\partial n_0/\partial r$, $\mathcal{E}_r \equiv E_r/v_s B$, and $\bar{\lambda} \equiv 1 + \lambda$. For simplicity we assume that δ/r and $\mathcal{E}_r/r$ are constant, so that both the ion and electron fluids rotate as solid bodies. Then we can define uniform rotation frequencies $\Omega_0 \equiv v_{\theta 0}/r$ and $\Omega_{0e} \equiv v_{e\theta 0}/r$, given by

$$\Omega_0(1 + \Omega_0) = (\lambda\delta - \mathcal{E}_r)/r, \quad \Omega_{0e} = -(\delta + \mathcal{E}_r)/r. \tag{7}$$

This assumption justifies our neglect of $\mathbf{\Pi}_0$, since the shear in $\mathbf{v}_0$, $\mathbf{v}_{0e}$ now occurs only in the small classical diffusion velocities[5] given in Eq. (6). From Eq. (7) one finds that the uniformity of Ω_{0e} requires n_0 to be of the form

$$n_0 = n_{00}\exp\left[-\tfrac{1}{2}r^2(\Omega_{0e} + \mathcal{E}_r/r)\right] = n_{00}\exp(-r^2/r_0^2), \tag{8}$$

with

$$r_0^2 \equiv -2r/\delta = \text{const}.$$

Clearly, if $|\mathcal{E}_r| \gg |\delta|$, the condition on n_0 is not a strong one, and our results will be valid for arbitrary distributions $n_0(r)$ as long as $\mathcal{E}_r/r$ is constant.

Next we linearize Eqs. (1)–(3) under perturbations of the form $\chi_1 = \chi(r)\exp i(m\theta + \kappa_\parallel z - \Omega\tau)$ and $\nu = \nu(r)\exp i(m\theta + \kappa_\parallel z - \Omega\tau)$, where $\nu \equiv n_1(r)/n_0(r)$, $\kappa_\parallel \equiv k_\parallel a$, and $\Omega \equiv \omega/\omega_c$. The electron equations can easily be solved if we neglect v_z and $\eta_\perp$, as previously indicated; we then obtain the relation

$$\psi_e\nu + (\delta\gamma - i\epsilon^{-1}\kappa_\parallel^2)(\chi - \nu) = 0, \tag{9}$$

where $\psi_e \equiv \Omega - m\Omega_{0e}$ and $\gamma \equiv m/r$. The linearized form of Eq. (1) for the ions can be written

$$-i\Omega\mathbf{v} + (\mathbf{v}\cdot\nabla\mathbf{v}_0 + \mathbf{v}_0\cdot\nabla\mathbf{v}) = -\nabla\chi - \lambda\nabla\nu + \mathbf{v}\times\hat{\mathbf{z}} + \lambda\mathbf{P}, \tag{10}$$

where we have neglected the resistance term and suppressed the subscript 1. $\mathbf{P}$ is defined by

$$\mathbf{P} = -[\nabla\cdot\mathbf{\Pi} + \mathbf{\Pi}\cdot(\nabla n/n)]_1. \tag{11}$$

As shown in Appendix I, the collision-independent part of $\mathbf{P}$ can be written $\mathbf{P} = \mathbf{A}\cdot\mathbf{v}$, where $\mathbf{A}$ is a dyadic operator,

$$A_{rr} = A_{\theta\theta} = i\gamma\left(\frac{1}{2}\delta + \frac{1}{r}\right), \quad A_{r\theta} = -A_{\theta r} = \frac{1}{2}\left(\frac{\partial^2}{\partial r^2} - \gamma^2\right) + \frac{1}{2}\left(\delta + \frac{1}{r}\right)\left(\frac{\partial}{\partial r} - \frac{1}{r}\right). \tag{12}$$

The r and θ components of Eq. (10) are, respectively,

$$-i(\Omega - m\Omega_0)v_r - 2\Omega_0 v_\theta + v_r v_{r0}' + v_{r0}v_r' = -(\chi + \lambda\nu)' + v_\theta + \lambda P_r, \tag{13}$$

[5] Note that the centrifugal force causes v_{r0} to differ from v_{er0}, and hence a classical mobility exists even for a fully ionized plasma. If $\mathcal{E}_r \gg \lambda\delta$ and $\Omega_0 \ll 1$, Eq. (6) yields $v_{r0} - v_{er0} \approx -2\bar{\lambda}\epsilon\delta\,\mathcal{E}_r/r$. This is usually too small to be experimentally significant.

$$-i(\Omega - m\Omega_0)v_\theta + v_r v'_{\theta 0} + \frac{1}{r} v_r v_{\theta 0} + v_{r0} v'_\theta + \frac{1}{r} v_{r0} v_\theta$$
$$= -i\gamma(\chi + \lambda\nu) - v_r + \lambda P_\theta, \tag{14}$$

where the prime indicates $\partial/\partial r$. We shall neglect v_z, which is negligible compared to v_{ez}, so that the z component of Eq. (10) is not needed. In Eq. (14) the terms $v_r v'_{\theta 0}$ and $v_r v_{\theta 0}/r$ coming from the $\mathbf{v}\cdot\nabla\mathbf{v}_0$ term and the Coriolis force, respectively, combine to give $2\Omega_0 v_r$, as a consequence of the definition of Ω_0. A similar term $-2\Omega_0 v_\theta$ in Eq. (13) is the first-order centrifugal force. These terms give rise to a factor $C \equiv 1 + 2\Omega_0$, which appears repeatedly in what follows. To keep track of these effects, we write as C_1 that factor due to centrifugal force and as C_2 that factor due to Coriolis force and its companion term, where $C_1 = C_2 = 1 + 2\Omega_0$.

Defining $\psi \equiv \Omega - m\Omega_0$ and $\Phi = \chi + \lambda\nu$, we obtain from Eqs. (12)–(14) a pair of coupled second-order differential equations for v_r and v_θ for the case of negligible ion–ion collisions,

$$iL_1 v_r + (C_1 + L_2)v_\theta = \Phi', \tag{15}$$

$$iL_1 v_\theta - (C_2 + L_2)v_r = i\gamma\Phi, \tag{16}$$

where L_1 and L_2 are the linear operators

$$L_1 = \psi + \lambda m(r^{-2} - r_0^{-2}), \tag{17}$$

$$L_2 = \left[\frac{\lambda}{2}\frac{\partial^2}{\partial r^2} - \frac{m^2}{r^2} - \left(\frac{1}{r^2} - \frac{2}{r_0^2}\right)\left(1 - r\frac{\partial}{\partial r}\right)\right]. \tag{18}$$

In the absence of collisional viscosity, only L_2 is differential. The linearized form of the ion continuity Eq. (3) is

$$\psi\nu - \gamma v_\theta + i\left(\delta + \frac{1}{r}\right)v_r + iv'_r = 0. \tag{19}$$

The eigenvalue equation for Ω is obtained by inserting the solution of Eqs. (15) and (16) for $\mathbf{v}(\Phi)$ into Eq. (19) and substituting for Φ the expression found from the electron equation (9). The destabilizing term due to zero-order centrifugal force will then appear from the difference between the Doppler-shifted frequencies ψ and ψ_e; from Eq. (5) this difference is seen to be proportional to Ω_0^2.

In some mirror-confined plasmas of low density and high temperature the assumption of quasineutrality breaks down, and finite Debye-length effects play a role. These effects are computed in Appendix II.

III. SOLUTION FOR SMALL ROTATIONS AND $k_z = 0$

Small Larmor Radius Expansion

To solve Eqs. (15)–(18) for $\mathbf{v}(\Phi)$, we make an expansion in the small parameter $\rho \equiv a/l$, where l is the scale length of macroscopic gradients. Since r and r_0 are measured in units of a, Eq. (17) gives $L_2 = O(\rho^2)$. By small rotations we mean values of E_r such that $\psi = O(\rho^2)$; then L_1 is also of $O(\rho^2)$. Clearly, an expansion in powers of ρ will break down for values of m such that $\gamma = (m/r) \approx 1$; similarly, the expansion will break down for radial wavelengths of order a. Multiplying Eq. (15) by L_1, operating on Eq. (16) by $C_1 + L_2$, subtracting, and retaining terms of $O(\rho^3)$ or larger, we obtain an equation for v_r alone. The commutator $(L_1L_2 - L_2L_1)$ is of $O(\rho^4)$ and is dropped. The complementary procedure yields an equation for v_θ. We thus obtain the separated equations

$$[C_1C_2 + (C_1 + C_2)L_2]v_r$$
$$= iL_1\Phi' - i(C_1 + L_2)(\gamma\Phi), \tag{20}$$

$$[C_1C_2 + (C_1 + C_2)L_2]v_\theta$$
$$= (C_2 + L_2)\Phi' - L_1\gamma\Phi. \tag{21}$$

If we write $\mathbf{v} = \mathbf{v}^{(0)} + \mathbf{v}^{(1)}$, where $\mathbf{v}^{(1)} = O(\rho^2)\mathbf{v}^{(0)}$, Eqs. (20) and (21) may be solved order by order without integration. We then obtain

$$iC^2 v_r = (C - L_2)(\gamma\Phi) - L_1\Phi', \tag{22}$$

$$C^2 v_\theta = (C - L_2)\Phi' - L_1\gamma\Phi, \tag{23}$$

where for brevity we have dropped the distinction between C_1 and C_2. Carrying out the operations indicated in Eqs. (22) and (23) and substituting the result into Eq. (19), we find that a large number of terms cancel out, including the coefficient of Φ'''. The first term in Eq. (19) can be put in terms of Φ by use of the electron equation (9); for $k_z = 0$ this gives

$$\nu = -\delta\gamma\Phi/(\psi - m\Omega_0^2), \tag{24}$$

where we have used the relation $\psi_e = \psi + \gamma(\bar{\lambda}\delta - r\Omega_0^2)$. We finally obtain from Eq. (19) a second-order differential equation for $\Phi \equiv \chi + \lambda\nu$,

$$\Phi'' + \left(\frac{1}{r} - \frac{2r}{r_0^2}\right)\Phi' - \frac{m^2}{r^2}\Phi + \frac{2}{r_0^2}N\Phi = 0, \tag{25}$$

where

$$N = -m\Omega_0\frac{2\psi(1 + 2\Omega_0 + \lambda r_0^{-2}\Omega_0^{-1}) + m\Omega_0(1 + 2\Omega_0 - 2\lambda r_0^{-2})}{(\psi - 2\lambda m r_0^{-2})(\psi - m\Omega_0^2)}. \tag{26}$$

N is a constant in virtue of the assumed uniformity of Ω_0 and r_0.

Solution of Whittaker's Equation

Following the procedure of Ref. 1, we can put Eq. (25) into standard form by the transformation

$$\Phi = z^{-\frac{1}{2}}e^{\frac{1}{2}z}W(z), \qquad z = r^2/r_0^2, \tag{27}$$

whereupon it becomes Whittaker's equation,[6]

$$(d^2W/dz^2) + \{-\tfrac{1}{4} + (p/z) + [(\tfrac{1}{4} - q^2)/z^2]\}W = 0, \tag{28}$$

with $p = \frac{1}{2}(1 + N)$, $q = \frac{1}{2}m$. The solution of this which vanishes at $z = 0$ is given by Kummer's function $M_{p,q}(z)$, which for $q > 0$ has the series expansion[6]

$$M_{p,q}(z) = z^{q+\frac{1}{2}}e^{-\frac{1}{2}z}\left[1 + \frac{\frac{1}{2} + q - p}{1!\,(2q+1)}z + \frac{(\frac{1}{2} + q - p)(\frac{3}{2} + q - p)}{2!\,(2q+1)(2q+2)}z^2 + \cdots\right]. \tag{29}$$

If the other boundary condition is $M_{p,q}(Z) = 0$, then if $Z \ll 1$ the eigenvalue of p is approximately $p = (1 + m)(\frac{1}{2} + Z^{-1})$, obtained from the first two terms of the series. On the other hand, if $Z \gg 1$, $M_{p,q}(z)$ is exponentially decreasing at large z if and only if the series terminates; this requires $p = q + \frac{1}{2} + n$ or $N = 2n + m$, where $n = 0, 1, 2, \cdots$, is the radial wavenumber. This eigenvalue, obtained by Rosenbluth *et al.*,[1] is independent of $Z = R^2/r_0^2$ and is not necessarily accurate because Z is not very large in practical situations; furthermore, Φ does not decrease exponentially when $M_{p,q}(z)$ does. However, if we adopt this eigenvalue for convenience, Eq. (26) then yields the quadratic dispersion equation

$$\psi^2 + \left[-\frac{2\lambda m}{r_0^2}\left(1 - \frac{1}{N}\right) - m\Omega_0^2\left(1 - \frac{4}{N}\right) + \frac{2m\Omega_0}{N}\right]\psi + m\Omega_0^2\left[\frac{m}{N}(1 + 2\Omega_0) + \frac{2\lambda m}{r_0^2}\left(1 - \frac{1}{N}\right)\right] = 0, \tag{30}$$

where N is a positive real number approximated by $2n + m$.

To recover the stability criterion of Ref. 1, we set $\lambda = 1$ and neglect all terms in Ω_0^2 except the leading term in the last bracket; we then obtain

$$N\psi^2 + [(1 - N)(2m/r_0^2) + 2m\Omega_0]\psi + m^2\Omega_0^2 = 0. \tag{31}$$

For $N = m = 1$, ψ is clearly real. For $N > 1$, the condition that the discriminant be positive, and hence ψ real, works out to be

$$-(N^{\frac{1}{2}} + 1) < r_0^2\Omega_0 < (N^{\frac{1}{2}} - 1). \tag{32}$$

Remembering from Eq. (5) that $\Omega_0 \approx (\delta - \mathcal{E}_r)/r = -(2/r_0^2) - (\mathcal{E}_r/r)$, we find stability when

$$\tfrac{1}{2}(1 - N^{\frac{1}{2}}) < (\mathcal{E}_r/\delta) < \tfrac{1}{2}(1 + N^{\frac{1}{2}}). \tag{33}$$

This is identical to the criterion of Ref. 1 because $\mathcal{E}_r/\delta$ is equal to the ratio W/W_i appearing there. The validity of Eq. (30) is limited by $\psi = O(\rho^2)$, which from the solution of Eq. (30) requires $\Omega_0 \leq O(r_0^{-2})$. For such small rotations Eq. (31) is sufficiently accurate. Extension to larger values of Ω_0 is accomplished in Sec. IV. We note, however, that whereas Eq. (31) predicts stability for $N = 1$, Eq. (30) predicts instability for $N = 1$, $\Omega_0 < 0$, with a growth rate $\text{Im}\,\Omega = O(\rho^3)$ if $\Omega_0 = O(\rho^2)$.

Physical Interpretation

The first term in the coefficient of ψ in Eq. (30) or (31) is the usual finite-r_L stabilization term. It vanishes if $\lambda = T_i/T_e = 0$ or $m/r_0^2 \propto \kappa_\perp\delta \to 0$. As pointed out previously,[1] it also vanishes if $N = 1$ because for $n = 0$, $m = 1$, the perturbed electric field is uniform, and no difference in ion and electron E/B drifts can occur.

The term proportional to Ω_0 in the coefficient of ψ is the one which causes the asymmetry in the stability criterion (32). An asymmetry in Eq. (33) is expected, since an $\mathcal{E}_r > 0$ adds to the rotation due to the pressure gradient $\delta < 0$, whereas an $\mathcal{E}_r < 0$ reduces it. Equation (32) shows, however, that the criterion is not symmetric even in the total rotation velocity Ω_0. If one had kept separate the factors C_1 and C_2 subsequent to Eq. (21), one would have found that the term causing the asymmetry arises not from C_1 but from C_2, that is, from the Coriolis force and its companion term in Eq. (14). The physical reason for this effect is that the Coriolis force $-v_r\Omega_0\hat{\boldsymbol{\theta}}$ causes a drift in the r direction which can either aid or oppose a similar drift due to the finite-r_L effect. From Eq. (31) it is clear that the Ω_0 term aids finite-r_L stabilization if $\Omega_0 < 0$ and vice versa. Consequently, in Eq. (32) the stable region is larger for $\Omega_0 < 0$ than for $\Omega_0 > 0$. The net result is that the asymmetry in the condition (33) on $\mathcal{E}_r$ is reduced to half of what it would be if it were due entirely to the effect noted at the beginning of this paragraph.

[6] E. T. Whittaker and G. N. Watson, *A Course of Modern Analysis* (Cambridge University Press, Cambridge, 1952), 4th ed., p. 337.

Solution by the Wentzel–Kramers–Brillouin Method

Equation (28) is in the standard form for the phase-integral (Wentzel–Kramers–Brillouin) method[7]

$$W'' + Q(z)W = 0, \tag{34}$$

except that $Q(z)$ is singular at the origin. Since this method is often used for the case $k_\parallel \neq 0$, we wish to check the accuracy of the method for the case $k_\parallel = 0$, where an exact solution is possible. Since

$$Q(z) = -\tfrac{1}{4} + [(1+N)/2z] + [(1-m^2)/4z^2], \tag{35}$$

the turning points $Q(z_{1,2}) = 0$ occur at $z_{1,2} = 1 + N \pm [(1+N)^2 + 1 - m^2]^{\frac{1}{2}}$. If N is real and $N \geq m > 1$, then z_1 and z_2 are positive; and Q is positive between the turning points and negative outside. We can then match an oscillatory solution between z_1 and z_2 to exponentially decaying solutions outside by the usual quantization condition

$$\int_{z_1}^{z_2} Q^{\frac{1}{2}}(z)\, dz = (n + \tfrac{1}{2})\pi. \tag{36}$$

The integration can be carried out with standard formulas; this yields

$$N = 2n + (m^2 - 1)^{\frac{1}{2}}, \tag{37}$$

to be compared with $N = 2n + m$, obtained from the solution of Whittaker's equation. Thus the WKB solution is quite accurate even for $m = 2$. The WKB method is useless for $m = 1$ because there is only one turning point. The reason the singularity in Q is not harmful for $m > 1$ is that Q is large and negative near the origin, and the solution decays very rapidly for $z < z_1$, so that the behavior at $z = 0$ is irrelevant. Note that the agreement between Eq. (37) and the exact result applies only to cases where $Z \gg 1$; the eigenvalue for practical cases where $Z = O(1)$ can be found only numerically.

If we had chosen N to be complex, the turning points would have been complex, and Eq. (36) should be interpreted as the path-independent line integral in the complex z plane between z_1 and z_2. As long as $Q(z)$ is not explicitly complex, the real and imaginary parts of Eq. (36) would yield the result that N, z_1 and z_2 must indeed be real; and ψ must be complex to make them so.

IV. SOLUTION FOR LARGE ROTATIONS AND $k_\parallel = 0$

To extend the calculation to larger values of $\mathcal{E}_r$ and Ω_0, we must consider $\psi \neq O(\rho^2)$. If we let $\psi = O(1)$ in Eq. (17), L_1 is no longer of $O(\rho^2)$ but can be written $L_1 = \psi + L_3$, where $L_3 = O(\rho^2)$. We can then follow the same procedure as before, solving Eqs. (15) and (16) order by order for $\mathbf{v}$ in terms of Φ, and inserting $\mathbf{v}(\Phi)$ and $\nu(\Phi)$ from Eq. (24) into Eq. (19). After considerable algebra, we then obtain a rather cumbersome fourth-order differential equation for Φ, which we shall not write down. If one assumes $\psi = O(\rho)$, however, the third and fourth derivatives of Φ may be neglected, and one again obtains Eq. (25) but with some additional terms in N. The transformation into Whittaker's equation and its solution are the same as before, so that for $\psi = O(\rho)$ the dispersion relation is given by

$$-N = -(2n+m) = m \cdot \frac{\psi(C^2 - 2\psi^2) + (\psi - m\Omega_0^2)(-C + 2\lambda r_0^{-2} + C^{-1}\psi^2)}{(\psi - 2\lambda m r_0^{-2})(\psi - m\Omega_0^2)}. \tag{38}$$

Since $C \equiv 1 + 2\Omega_0$, this is seen to be identical with Eq. (26) except for the terms containing ψ^2 explicitly.

Equation (38) is a cubic in ψ, which for $\lambda = 1$ and $n = 0$ can be written

$$-\rho^2 m^2 \Psi^3 + (1 - m\rho^4 s^2) m \Psi^2 + [1 - m + 2s + \rho^2 s^2(4 - m)]\Psi + s^2[1 + \rho^2(2s + m - 1)] = 0, \tag{39}$$

where $\rho^2 \equiv 2/r_0^2$, $s \equiv \Omega_0/\rho^2$, and $\Psi = \psi/m\rho^2$. We have also replaced C^{-1} in the last term of the numerator of Eq. (38) by 1, which is legitimate for $|\Omega_0| \ll 1$. Equation (39) has been solved numerically for $r_0 = 58$, corresponding to a typical stellarator plasma, and for $r_0 = 10$, corresponding to a typical cesium plasma.

In Fig. 1 are shown the stability limits according to the cubic equation (39) and the appropriate quadratic equation (31). It is seen that the simple stability criterion (33) is very accurate even for $|\mathcal{E}_r/\delta| > 1$. The assumption $\psi = O(\rho)$ breaks down for values of $|\mathcal{E}_r/\delta|$ larger than shown on Fig. 1; for larger rotations, the fourth-order differential equation has to be solved. In general, for larger rotations finite-r_L stabilization sets in at values of m smaller than is indicated by Eq. (31) or (39). In Fig. 2 is shown the growth rate Im Ω vs m for various values of $\mathcal{E}_r/|\delta|$, the ratio of E/B drift to diamagnetic drift. Curiously, the region of stability is centered around a small negative value *either* of $\mathcal{E}_r$ *or* of $r\Omega_0 \approx -|\delta| - \mathcal{E}_r$. The growth rate seems to vary inversely with $|\delta|$, but this is a consequence of the assumed shape of $n_0(r)$, which simply requires the instability

[7] J. Heading, *An Introduction to Phase-Integral Methods* (John Wiley & Sons, Inc., New York, 1962).

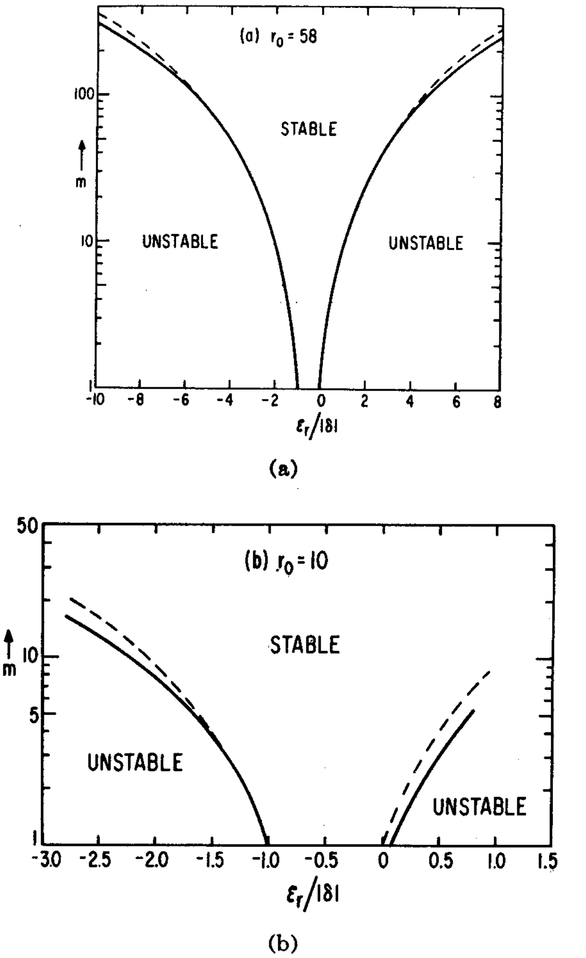

FIG. 1. Stability limits for the lowest radial mode according to the cubic equation (39) (solid curve) and the approximate quadratic equation (31) (dashed curve), for (a) $r_0 = 58$ and (b) $r_0 = 10$, where r_0 is essentially the plasma radius in units of the Larmor radius. $\mathcal{E}_r/|\delta|$ is the ratio of E/B drift velocity to the magnitude of the diamagnetic drift velocity (for $T_i = T_e$), and m is the azimuthal mode number.

to occur at larger r if r_0 is increased. The *local* growth rate, of course, is proportional to $|\delta|$ and vanishes if $|\delta| \to 0$. The dashed curves in Fig. 1 are valid for $n \neq 0$ if m is simply replaced by $N = 2n + m$. From this it is clear that increasing the radial wavenumber increases the finite-r_L stabilization, so that the frequency spectrum will be shifted toward the low-frequency end if n is increased.

V. EXTENSION TO FINITE $k_\parallel$

The Radial Equation

We now consider finite but small values of $k_\parallel$ such that ion motions parallel to **B** may still be neglected; the condition found previously[4] for this is $k_\parallel^2/k_\perp^2 \ll \delta^2$. If electron motion along **B** is controlled by collisions with ions, as is the case when $\epsilon \gg (m_e/m_i)$, Eq. (9) is the proper equation of continuity for the electrons. The ion velocity $\boldsymbol{v}$ is the same as before, but into the ion equation of continuity (19) we must now insert

$$\nu(\Phi) = -\frac{\delta\gamma - i\epsilon^{-1}\kappa_\parallel^2}{\psi - m\Omega_0^2 + i\lambda\epsilon^{-1}\kappa_\parallel^2}, \qquad (40)$$

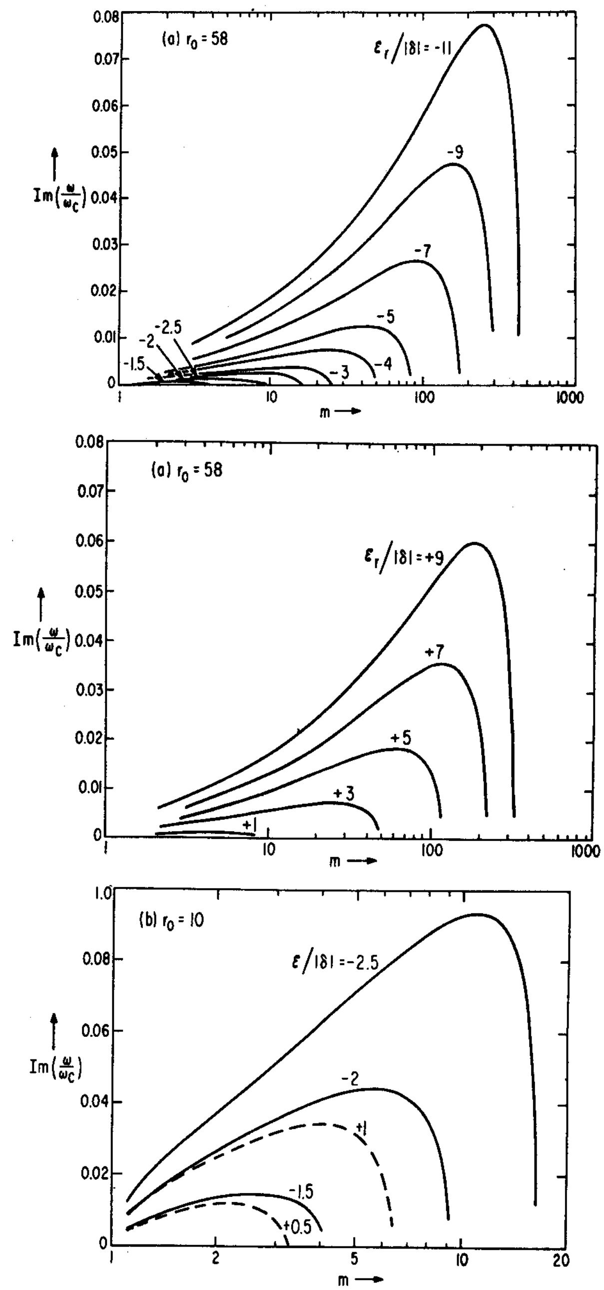

FIG. 2. Growth rates versus m-number, computed from Eq. (39), for various values of the normalized electric field $\mathcal{E}_r/|\delta|$, for (a) $r_0 = 58$ and (b) $r_0 = 10$. The growth rates generally increase with m but cut off sharply when finite-r_L stabilization sets in.

found from Eq. (9), instead of Eq. (24). We then obtain Eq. (25), in which N is now a function of r. For $\psi = O(\rho)$, $N(r)$ is given by

$$N(r) = \frac{\psi(2\psi^2 - C^2)[m + i\rho^{-2}f(r)] + m(C - \lambda\rho^2 - C^{-1}\psi^2)[\psi - m\Omega_0^2 + i\bar{\lambda}f(r)]}{(\psi - \lambda m\rho^2)[\psi - m\Omega_0^2 + i\bar{\lambda}f(r)]}, \quad (41)$$

$$f(r) \equiv \epsilon^{-1}\kappa_\parallel^2 = B\kappa_\parallel^2(r)/[e\eta n_0(r)]. \quad (42)$$

Using the transformation (27) and simplifying $N(r)$ by restricting ourselves to $\psi = O(\rho^2)$, we finally obtain

$$W'' + Q(z)W = W'' + \left[-\frac{1}{4} + \frac{1 + N(z)}{2z} + \frac{1 - m^2}{4z^2}\right]W = 0, \quad (43)$$

where

$$-N(z) = \frac{\Psi(\lambda + 2s) + s^2 + i(\Psi - \bar{\lambda})g(z)}{\Psi(\Psi - \lambda)}, \quad (44)$$

$$g(z) = (B/n_{00}e\eta)[e^z\kappa_\parallel^2(z)/m\rho^4], \quad (45)$$

$\Psi = \psi/m\rho^2$, $s = \Omega_0/\rho^2$, and $\rho^2 = 2/r_0^2$. We have used Eq. (8) for the form of n_0. In this section we consider magnetic fields without shear, so that $\kappa_\parallel$ is constant.

From Eq. (44) it is clear that $N(z)$ cannot be made real at all z by any choice of Ψ; hence, $N(z)$ and $Q(z)$ are complex functions of z. Equation (43) is therefore in the form of Schrödinger's equation with a complex potential energy. This type of equation always arises in the theory of universal instabilities and is customarily solved by the complex WKB method.[8]

Local Dispersion Relation

If the radial wavelength is much larger than the azimuthal wavelength, the local growth rate at each radius can be estimated by neglecting the radial derivatives in Eq. (25) and using Eq. (44) for N. This yields the following algebraic equation for ψ:

$$\psi^2 + [\lambda\delta\gamma(1 + \delta\gamma^{-2}r^{-1}) - 2\delta\gamma^{-1}\Omega_0 + iY]\psi - \delta\gamma^{-1}m\Omega_0^2 + i\bar{\lambda}\delta\gamma Y = 0, \quad (46)$$

where $Y \equiv \kappa_\parallel^2/\epsilon\gamma^2$ and δ and γ, defined previously, are the local density gradient and azimuthal wavenumber. Setting $Y = 0$ yields the local growth rate for the centrifugal, or "gravitational," mode discussed in Sec. III. If $Y > O(\rho^2)$, we can expand the solution of Eq. (46) to obtain the local complex frequency ψ for the drift, or "universal," mode. This is

$$\psi = -\bar{\lambda}\delta\gamma + iY^{-1} \cdot\{\bar{\lambda}\delta^2\gamma^2[1 + \gamma^{-2}(\lambda\delta/r - 2\mathcal{E}_r/r)] - \delta r\Omega_0^2\}. \quad (47)$$

The last term in the curly brackets is simply the "gravitational" growth rate found previously,[4] but with the centrifugal force Mnv_0^2/r replacing the effective gravitational force $\bar{\lambda}nKT_e/R$ in a curved magnetic field. The first term in the curly brackets is the usual growth rate for the "universal" resistive overstability[4] (resistive drift mode), modified by some geometrical and Coriolis effects which vanish in the limit $r \to \infty$.

The effect of radial variations can be estimated by replacing the radial derivative by $i\kappa_r$, where κ_r is the local radial wavenumber. It is convenient to do this in Eqs. (43) and (44), which give

$$\Psi^2 + [-\lambda + N^{-1}(\lambda + 2s + ig)]\Psi + N^{-1}(s^2 - i\bar{\lambda}g) = 0, \quad (48)$$

in which, since $\kappa_z^2 \equiv -\partial^2/\partial z^2 = \kappa_r^2/2z\rho^2$,

$$N = [(m^2 - 1)/2z] + (\kappa_r^2/\rho^2) + \tfrac{1}{2}z - 1. \quad (49)$$

For the drift mode (large g), we have

$$\Psi = \bar{\lambda} + ig^{-1}[\bar{\lambda}(N + \lambda + 2s) + s^2]. \quad (50)$$

This is equivalent to Eq. (47) if $N = m^2/2z$. Note that because of the transformation Eq. (27), Eq. (46) is not exactly the same as the equation for the turning points of Eq. (43), as it would be in plane geometry.

From Eq. (50) we note the following: (1) $\mathrm{Re}\,\Psi = \bar{\lambda}$, so the wave travels at the electron diamagnetic drift velocity; (2) the gravitational part of the growth rate is independent of N, and hence of κ_r; (3) the universal part of Im Ψ is proportional to N, and hence to κ_r^2 if $\kappa_r \gg (m/r)$. This is opposite to the behavior of the centrifugal mode of Eq. (31), where the growth rate decreases with radial wavenumber n. The reason is that the drift mode is excited by finite-r_L effects whereas the gravitational mode is damped by them, as shown in a previous paper.[9]

Wentzel–Kramers–Brillouin Approximation

Formal application of the WKB method to Eqs. (43)–(45) gives the quantization condition

$$\int_{z_1}^{z_2}\left[-\frac{1}{4} + \frac{A_1 + iA_2\exp z}{2z} + \frac{1 - m^2}{4z^2}\right]^{\frac{1}{2}} dz = (n + \tfrac{1}{2})\pi, \quad (51)$$

[8] A. A. Galeev, Zh. Eksperim. i Teor. Fiz. 44, 1920 (1963) [English transl.: Soviet Phys.—JETP 17, 1292 (1963)].

[9] F. F. Chen, Phys. Fluids 8, 912 (1965).

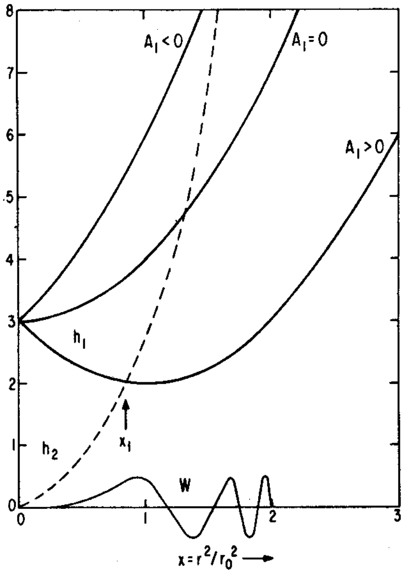

FIG. 3. Schematic of the curves h_1 and h_2, whose intersection gives the turning point x_1 for the drift mode, for three values of A_1 and one value of A_2. The coefficient of h_2 is proportional to the growth rate. The behavior of the wave function W is illustrated for the case $A_1 > 0$ and $X = 2$, X being the boundary.

where

$$A_1 = 1 - [\Psi(\lambda + 2s) + s^2]/[\Psi(\Psi - \lambda)], \tag{52}$$

$$A_2 = (\kappa_\parallel^2/\epsilon_0 m\rho^4)\{(\Psi - \bar{\lambda})/[\Psi(\Psi - \lambda)]\}, \tag{53}$$

and ϵ_0 is the normalized resistivity at $r = 0$. The dependence of ϵ on density, which varies exponentially, is shown explicitly in Eq. (51). The integral in Eq. (51) between the complex turning points z_1 and z_2 is independent of path, and the real and imaginary parts of that equation give, in principle, two equations for the real and imaginary parts of Ψ. Once the eigenvalue of Ψ is found, the finiteness of the solution at 0 and ∞ can be checked by computing the antistokes lines defined by Im $\int_{z_{1,2}}^{z} Q^{\frac{1}{2}}\,dz = 0$ and seeing whether or not they cross the real axis; if so, the solution is exponentially decaying at small and large radii. Clearly, the Wentzel–Kramers–Brillouin method is not very useful here because the integral in Eq. (51) is intractable, and even the turning points cannot be expressed simply in terms of Ψ because the equation $Q = 0$ is transcendental. The integral cannot be evaluated numerically until Ψ is known, so that in general a trial and error process is necessary; in such a case one may as well solve the original equation (43) numerically.

We can, however, make some progress with the drift mode occurring at "large" values of $\kappa_\parallel$. If one assumes $\Psi^i \ll \Psi^r$, where the superscripts indicate the imaginary and real parts, then A_1 is essentially real. If one further assumes that Q is nearly real, then the turning points $z_{1,2} = x_{1,2} + iy_{1,2}$ are nearly real, and the integral in Eq. (51) can be approximated by an integral along the real axis. This requires A_2 to be nearly imaginary; from Eq. (53) we see that this happens when either $\kappa_\parallel^2 \approx 0$ or $\Psi \approx \bar{\lambda}$. The former corresponds to the centrifugal mode of Sec. III; the latter to the drift mode we are considering here. Setting $\Psi^r = \bar{\lambda}$, we find for the real part of Eq. (51)

$$\int_{x_1}^{x_2} \left[-\frac{1}{4} + \frac{A_1 + A_2 e^x}{2x} + \frac{1 - m^2}{4x^2} \right]^{\frac{1}{2}} dx = (n + \tfrac{1}{2})\pi, \tag{54}$$

where

$$A_1 = 1 - [\lambda + 2s + (s^2/\bar{\lambda})], \tag{55}$$

$$A_2 = (\kappa_\parallel^2/\epsilon_0 m\rho^4)\Psi^i/\bar{\lambda}. \tag{56}$$

The turning points occur at the intersections of the curves

$$h_1(x) = x^2 - 2A_1 x + m^2 - 1, \tag{57}$$

$$h_2(x) = 2A_2 x e^x. \tag{58}$$

In general, there is only one intersection and hence only one turning point.

Consider first the case $m \geq 2$. The curves $h_1(x)$ and $h_2(x)$ are shown schematically in Fig. 3 for different values of A_1. For more than one turning point to exist, A_1 must be larger than that value which makes the h_1 and h_2 curves tangent. Remembering that $x \equiv r^2/r_0^2 \geq 0$, we are then led to the approximate condition $A_1 > (m^2 - 1)^{\frac{1}{2}}$. From Eq. (55) we see that A_1 has a maximum of 2 at $s = -\bar{\lambda}$. Thus for $m = 2$ it is barely possible for three turning points to exist. Except for the case $m = 2$, $A \approx 2$, there exists only one turning point x_1 for $m \geq 2$. To the right of x_1 the exponential term in Eq. (54) dominates and Q is positive; hence,

$$W \approx Q^{-\frac{1}{4}} \exp i \int_{x_1}^{x} Q^{\frac{1}{2}}\,dx$$

is oscillatory. To the left of x_1, Q is negative and W is exponential.

The drift mode, therefore, is not localized. If we require W to take on the subdominant solution for $x < x_1$, then by the usual connection formulas we find that W is a standing wave for $x > x_1$ and decays only slowly with x because of the factor $Q^{-\frac{1}{4}}$. This oscillatory solution must have a null at the boundary $x = X$ if the boundary is conducting. In practical devices the boundary is often defined by a conducting aperture limiter. If the device is not too long, the potential of the cylinder defined by the limiter is a constant determined by the sheath drop at the limiter; a conducting boundary is then a good approximation. Although localized solutions do not exist, the WKB condition (54) can still be used if x_2 is replaced by X. Moiseev and Sagdeev[10] found localized solutions for the resistive drift mode ($\mathcal{E}_r = 0$) by ignoring the exponential behavior of ϵ and expanding around the region where the density gradient is a maximum. However, it is inconsistent to assume that the perturbation is localized to a region where ϵ can be regarded as constant; it is precisely the fast-varying exponential term in Eq. (54) that makes it impossible to have a second turning point. Note that $\mathcal{E}_r = 0$ corresponds to $s = -1$ and $A_1 = \frac{3}{2}$ if $\lambda = 1$.

In retaining the exponential term we cannot obtain the usual solution in terms of Hermite polynomials. However, we can estimate the growth rate of the drift mode in certain cases. For large radial wavenumbers n, Ψ^i is approximated by assuming $X \gg x_1$, so that the exponential term dominates in most of the region of integration. The integral in Eq. (54) can then be evaluated, giving

$$(n + \tfrac{1}{2})\pi \approx \int_{x_1}^{X} \left(\frac{A_2 e^x}{2x}\right)^{\frac{1}{2}} dx = 2A_2^{\frac{1}{2}}[e^{\frac{1}{2}X}F(\tfrac{1}{2}X)^{\frac{1}{2}} - e^{\frac{1}{2}x_1}F(\tfrac{1}{2}x_1)^{\frac{1}{2}}],$$

where

$$F(t) \equiv e^{-t^2} \int_0^t e^{u^2}\, du.$$

The function $F(t)$, tabulated by Miller and Gordon,[11] has a broad maximum ≈ 0.54 at $x \approx 0.92$. Letting $F \approx 0.5$ and neglecting $\exp(\frac{1}{2}x_1)$ relative to $\exp(\frac{1}{2}X)$, we obtain $(n + \frac{1}{2})\pi \approx A_2^{\frac{1}{2}} \exp(\frac{1}{2}X)$, or

$$\Psi^i \approx \bar{\lambda}\epsilon_0 m\rho^4\kappa_\parallel^{-2}(n + \tfrac{1}{2})^2\pi^2 \exp(-X), \quad (\text{large } n). \quad (59)$$

This varies as n^2, in agreement with Eqs. (49) and (50), and is independent of s. The reason is that the gravitational part of the growth rate is diminished by finite-r_L effects at large values of n, leaving only the universal part. For small n, a lower limit on Ψ^i can be found by the condition $x_1 = X$. We then find

$$\Psi^i \gtrsim \tfrac{1}{2}\bar{\lambda}\epsilon_0 m\rho^4\kappa_\parallel^{-2}[X - 2A_1 + (m^2 - 1)/X] \cdot \exp(-X), \quad (60)$$

which does depend on A_1 and, hence, on s.

Consider now the case $m = 1$, for which the turning points are given by $x - 2A_1 = 2A_2e^x$. Remembering that $x \geq 0$ by definition, one can easily show that for $2 > A_1 > 0$, there are two turning points for $A_2 < \bar{A}_2$ and no turning points for $A_2 > \bar{A}_2$, where $\bar{A}_2 \equiv \frac{1}{2}\exp(-1 - 2A_1)$; for $0 > A_1 > -\frac{1}{2}$, there are two turning points for $\bar{A}_2 > A_2 > -A_1$, one turning point for $A_2 < -A_1$, and no turning points for $A_2 > \bar{A}_2$; for $A_1 < -\frac{1}{2}$, there is one turning point for $A_2 < -A_1$ and none for $A_2 > -A_1$. When there is one turning point, the situation is similar to the previous case of $m \geq 2$. When there are two turning points, a region of evanescence separates two regions of propagation; and when there are no turning points, the solution is oscillatory everywhere and is determined by the boundary conditions $W = 0$ at $x = 0$ and $x = X$. Equations (59) and (60) are still applicable in the limiting cases, and the growth rate increases with radial wavenumber.

In the general case when n and $\kappa_\parallel^2$ are not large enough for these approximate formulas to be valid and m is not large enough for the local dispersion relations to be accurate, Eqs. (43)–(45) must be solved numerically. Since the solution for a nonlocalized mode in cylindrical geometry is not usually given in the literature, we have performed this calculation for a few typical cases. The results will be given a subsequent paper.

VI. SHEAR STABILIZATION

General Remarks

We begin with a discussion of the mechanism of stabilization of drift-type instabilities by shear in the magnetic field, a subject previously treated by Mikhailovsky and Mikhailovskaya,[12] Galeev,[8] Stringer,[13] and Frieman.[14] Consider a magnetic field of the form $\mathbf{B} = B_z\hat{\mathbf{z}} + B_\theta(r)\hat{\boldsymbol{\theta}}$. Because of the shear, a perturbation with a given κ_z will have a different $\kappa_\parallel$ at each radius,

$$\kappa_\parallel(r) = \kappa_z + (m/r)B_\theta(r)/|B|. \quad (61)$$

This has the effect of localizing perturbations to a range of r in which $\kappa_\parallel$ does not vary widely. Only those perturbations with a sufficiently large effective radial wavenumber κ_r can then be excited. If the shear is sufficiently large, some modes are completely

[10] S. S. Moiseev and R. Z. Sagdeev, Zh. Techn. Fiz. SSSR 34, 248 (1964) [English transl.: Soviet Phys.—Tech. Phys. 9, 196 (1964)].

[11] W. L. Miller and A. R. Gordon, J. Phys. Chem. 35, 2875 (1931).

[12] L. V. Mikhailovskaya and A. B. Mikhailovsky, Nucl. Fusion 3, 28 (1963).

[13] T. E. Stringer, Princeton Plasma Physics Laboratory Report MATT-320 (1965).

[14] E. A. Frieman, K. Weimer, and P. Rutherford, in Second Conference on Plasma Physics and Controlled Nuclear Fusion (1965), Paper CN21/118.

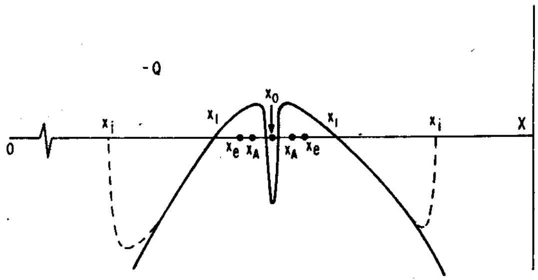

FIG. 4. Behavior of the effective potential energy $-Q$ with the coordinate x when the magnetic field possesses shear. The perturbation is parallel to the lines of force at $x = x_0$. Other symbols are defined in the text.

stabilized because the region of localization is smaller than the shortest possible radial wavelength.

There are several reasons for the localization of a given mode. One is that the "natural" turning points of the mode tend to come together when $\kappa_\parallel$ is a function of r. Localization also occurs because as $\kappa_\parallel$ is increased terms not normally included in the theory begin to be important and cause other turning points to appear. For instance, there is Landau damping. It is well known that the parallel phase velocity of drift waves lies in the range $v_{the} < \omega/k_\parallel < v_{thi}$, where v_{the} and v_{thi} are electron and ion thermal velocities, because otherwise the waves would be Landau damped. Since the waves cannot propagate outside this range, there must be turning points at radii where $k_\parallel \approx \omega/v_{thi}$ and $k_\parallel \approx \omega/v_{the}$. Furthermore, there must be turning points where $\kappa_r = k_r a \approx 1$, because the theory breaks down for wavelengths of the order of a ($\approx r_L$), and the mode cannot exist for $\kappa_r > 1$.

The situation is elucidated by Fig. 4, which is a schematic plot of the real part of the potential energy $-Q$ against the coordinate $x \equiv r^2/r_0^2$. We choose $\kappa_\parallel$ to be 0 at $x = x_0$ and assume that the shear is large enough that the points x_i, where $k_\parallel = \omega/v_{thi}$, lie between the axis $x = 0$ and the wall $x = X$. There is a narrow potential well near x_0, where the $\kappa_\parallel \approx 0$ mode of Sec. III can exist. This mode corresponds to the classical interchange instability, which at larger values of $\kappa_\parallel$ turns into an Alfvén wave. Surrounding this region is a potential barrier, in which the wave decays exponentially. Beyond the turning points x_1 are other potential wells in which the drift mode can exist. With ion Landau damping neglected, these wells deepen monotonically away from x_0; but, as Galeev[8] has shown, the ion damping term brings the curve back to the axis at x_i, somewhat as shown by the dashed lines. Thus the drift waves are localized between x_1 and x_i. The potential $-Q$ depends on the frequency Ψ; the outer wells exist only if $\Psi^i > 0$—that is, if the wave is overstable.

The points x_A and x_e are places where $\omega/k_\parallel = v_A$ (the Alfvén speed) and $\omega/k_\parallel = v_{the}$, respectively. In this paper we are concerned with $\beta < (m_e/m_i)$; this is equivalent to $v_A > v_{the}$. Therefore, as $\kappa_\parallel$ is decreased, the drift mode is affected by electron Landau damping before it is affected by the damping due to excitation of Alfvén waves. Thus the value of v_A, and hence of β, does not enter the problem, as one would expect at low β. Actually, the value of x_e, and hence of m_e/m_i, does not enter either, since in neglecting electron inertia we have assumed $\epsilon \gg (m_e/m_i)$, so that the value of x_1 depends only on ϵ. In unclosed systems with conducting endplates and in closed systems with a rotational transform the value of $\kappa_\parallel$ is limited from below, so that usually the center potential well does not exist at all. Then the entire region of nonelectrostatic, β-dependent phenomena is irrelevant, and the shear stabilization is independent of β. This picture is intuitively more satisfying than previous results,[8,12,14] which indicate a β dependence of the low-β shear stabilization criterion, because experiments on stellarators[15] indicate that for $\beta < (m_e/m_i)$ the confinement time is independent of β over several orders of magnitude.

To characterize the shear it is customary to define $\mu(r) \equiv B_\theta(r)/r\,|B|$, so that $\kappa_\parallel = \kappa_z + m\mu$ and $\kappa_\parallel' = m\mu'$. Here r and $\partial/\partial r$ are still normalized to the length $a \approx r_L$. The change of pitch angle of the lines of force over a distance r_0 is given by the dimensionless quantity $\theta \equiv |r\mu'|\, r_0$. In what follows, the radius $\bar{r} = x_0^{\frac{1}{2}} r_0$ at which $\kappa_\parallel$ is chosen to be zero is arbitrary. For definiteness we choose this to be the radius at which the density gradient is maximum; Eq. (8) then gives $\bar{r} = \rho^{-1}$ or $x_0 = \frac{1}{2}$. Then $\theta = r_0^2\,|\mu'|\,/\sqrt{2}$ and $\kappa_\parallel' = \sqrt{2} m\theta/r_0^2$. When the instability is sufficiently localized, we can expand $\kappa_\parallel(r)$ about $r = \bar{r}$: $\kappa_\parallel(r) = \kappa_\parallel'(\bar{r})(r - \bar{r}) + \cdots$, or $\kappa_\parallel(x) = \kappa_\parallel^*(x_0)(x - x_0) + \cdots$, where $\kappa_\parallel^* \equiv \partial\kappa_\parallel/\partial x = \kappa_\parallel'/r\rho^2$. This expansion is valid if $\frac{1}{2}\kappa_\parallel^{**}(x_0)(x_i - x_0) \ll \kappa_\parallel^*(x_0)$.

The point x_i is determined by the condition $\psi/\kappa_\parallel(x_i) = v_{thi}/v_s \approx \lambda^{\frac{1}{2}}$. For the drift mode, $\psi \approx \bar{\lambda} m\rho^2$, so that $x_i - x_0 \approx 2m\rho^2/\kappa_\parallel^*$ for $\lambda = 1$. Thus the validity of the expansion for $\kappa_\parallel$ is valid if $m\rho^2 \ll \kappa_\parallel^{*2}/\kappa_\parallel^{**}$, which is easily satisfied. The condition that the points x_i lie within the plasma is $|x_i - x_0| < x_0$ or $X - x_0$, whichever is less. If x_0 and $X - x_0$ are of $O(1)$, the above expressions for $x_i - x_0$ and $\kappa_\parallel^*$ yield

[15] W. Stodiek, J. O. Kessler, and D. J. Grove, Princeton Plasma Physics Laboratory Report MATT–Q–22 (1964), p. 79.

$$\theta > 4/r_0 \tag{62}$$

as the condition for this sort of localization.

Localized Modes

First we follow the usual procedure and look for highly localized modes whose amplitudes vanish at ∞. It is convenient to start from Eq. (25), with N given by Eqs. (44) and (45). We assume that the natural turning points are much closer together than the length r_0, so that the first derivative term in Eq. (25) can be neglected, and m/r can be replaced by $m/\bar{r}$. Further, we assume that $\kappa_\parallel(r)$ varies much more rapidly than exp $(-r^2/r_0^2)$, so that Eq. (45) can be written $g = g_0(r - \bar{r})^2$, where

$$g_0 \equiv (B/n_{00}e\eta)(e^{\bar{r}^2/r_0^2}/m\rho^4)\kappa_\parallel'^2(\bar{r}). \tag{63}$$

Equation (25) then becomes

$$\Phi'' + \left[-\frac{m^2}{\bar{r}^2} - \rho^2\frac{\Psi(\lambda + 2s) + s^2}{\Psi(\Psi - \lambda)} - i\rho^2 g_0\frac{(\Psi - \bar{\lambda})}{\Psi(\Psi - \lambda)}r^2\right]\Phi = 0, \tag{64}$$

where we have shifted the origin of r to $\bar{r}$. With the transformation

$$t = \left[\frac{4i\rho^2 g_0(\Psi - \bar{\lambda})}{\Psi(\Psi - \lambda)}\right]^{\frac{1}{4}} r, \tag{65}$$

this is put into the form of Weber's equation:

$$(\partial^2\Phi/\partial t^2) + (n + \tfrac{1}{2} - \tfrac{1}{4}t^2)\Phi = 0, \tag{66}$$

with

$$n + \tfrac{1}{2} = -\left(\frac{m^2}{\bar{r}^2} + \rho^2\frac{\Psi(\lambda + 2s) + s^2}{\Psi(\Psi - \lambda)}\right) \cdot \left(\frac{4i\rho^2 g_0(\Psi - \bar{\lambda})}{\Psi(\Psi - \lambda)}\right)^{-\frac{1}{2}}. \tag{67}$$

Solutions which vanish at ∞ have as eigenvalues $n = 0, 1, 2 \cdots$. Specializing to the case $\lambda = 1$ and $\bar{r} = 1/\rho$, we can write the dispersion relation (67) as follows:

$$m^4\Psi^4 - (2m^2p + i\bar{Y})\Psi^3 + (2m^2s^2 + p^2 + 3i\bar{Y})\Psi^2 - 2(s^2p + i\bar{Y})\Psi + s^4 = 0, \tag{68}$$

where

$$p \equiv m^2 - 1 - 2s, \qquad \bar{Y} \equiv (2n + 1)^2\kappa_\parallel'^2/\epsilon(\bar{r})m\rho^6.$$

We next separate Eq. (68) into real and imaginary parts and assume $\Psi^i \ll \Psi^r$ and $\bar{Y} \geq m^4$. The latter is a good assumption if $\theta = O(r_0^{-1})$ and $\epsilon < m^{-3}$. The imaginary part of Eq. (68) then reduces to $(\Psi^r - 1)(\Psi^r - 2) = 0$ or, for arbitrary λ,

$$(\Psi^r - \lambda)(\Psi^r - \bar{\lambda}) = 0.$$

The root $\Psi^r = \bar{\lambda}$ is the drift mode; and putting $\Psi^r = \bar{\lambda}$ into the real part of Eq. (68), we find that $\Psi^i < 0$. Thus the only localized drift mode is a stable one.

The root $\Psi^r = \lambda$ corresponds to a mode which is purely unstable in the frame in which $\mathcal{E}_r = 0$. The real part of Eq. (68) gives

$$\Psi^i = (s + 1)^2/\bar{Y}. \tag{69}$$

This is the only highly localized unstable mode and corresponds to the small center potential well in Fig. 4. Note that the universal mode $\mathcal{E}_r = 0$, $s = -1$, has neutral stability in this approximation. For $|\mathcal{E}_r| > 0$ there is no absolute stability, but the growth rate decreases with increasing shear. The turning points for this unstable mode can be determined now that Ψ is known; they lie on a 45° line through $\bar{r}$ in the complex r plane, and their separation is much larger than r_0 if $\theta \gg 2(s + 1)(2\epsilon/m)^{\frac{1}{2}}/r_0$. This is a much weaker condition than that given previously for the localization of the drift modes by ion Landau damping.

Of interest to an experimentalist is the ratio of growth rates with and without shear. For the centrifugal mode with $\kappa_\parallel \approx 0$, the growth rate Ω^i is found from Eq. (31). Comparing this with $m\rho^2\Psi^i$ by Eq. (69), we find for the lowest radial mode $n = 0$

$$\frac{\Omega^i\,(\text{shear})}{\Omega^i\,(\text{no shear})} = \frac{\epsilon\rho^6 T(s, m)}{\mu'^2}, \tag{70}$$

where ϵ and μ' are evaluated at $\bar{r}$, and T is an algebraic function of s and m. Typical values of T are shown in Table I.

TABLE I. Typical values of T.

s	m = 2	3	4	6	8	10
−2	0.38	0.19	0.13	0.086	0.095	∞
1	1.5	0.77	0.52	0.34	0.38	∞
+2	1.9	0.90	0.57	0.31	0.21	0.15

For $s = -1$, $T = 0$ because $\Omega^i = 0$ with shear. For $s = 0$ or $m = 1$ or for sufficiently large m, T is infinite because $\Omega^i = 0$ in the absence of shear; of course, this is only a consequence of our using the formula for $\kappa_\parallel$ exactly equal to zero for Ω^i in the absence of shear. From Table I one sees that high values of m are more greatly affected by shear. From the n dependence of Eq. (69) one sees that the higher radial modes are also more easily stabilized. Since

$T = O(1)$, the magnitude of shear necessary for an appreciable effect on the growth rate is, from Eq. (70), $|\mu'| > \epsilon^{\frac{1}{2}}\rho^3$ or

$$\theta > 2\epsilon^{\frac{1}{2}}/r_0. \qquad (71)$$

This is an extremely small shear. For example, if the shear is provided by a current I along the axis (hard core), then

$$\kappa_\parallel(r) = (2mI/aB)(r^{-2} - \bar{r}^{-2}), \qquad (72)$$

$$\theta = 8I/Br_0a, \qquad (73)$$

where I is in emu, B in Gauss, and r_0a in cm. Then Eq. (71) requires $I > \frac{1}{4}aB\epsilon^{\frac{1}{2}}$, which for a cesium plasma ($\epsilon \approx 10^{-4}$) at 4000 G means only 13 A in the hard core. Stabilization of this localized mode is therefore no problem in practice.

Once the eigenvalue problem is solved and Ψ is known, the antistokes lines can be computed. It is often supposed[8,13] that if the antistokes line does not cross the real axis as $r \to \infty$, the plasma is stable. However, all it means is that there are no localized solutions, such as the one discussed above, whose natural turning points lie well within the plasma. There still exists the possibility of nonlocalized unstable solutions which are oscillatory near the boundary and have a node at the boundary.

Nonlocalized Modes

We now consider the drift waves which can exist in the outer potential wells of Fig. 4. These overstable modes, discussed in Sec. V, are in general not localized in the absence of shear because they have only one turning point for $x > 0$. In the presence of shear, localization occurs only when Landau damping is taken into account. The amount of shear necessary is given by Eq. (62): $\theta > 4/r_0$. If the shear is weaker than this, it only modifies slightly the theory given by Eqs. (54)–(60) for zero shear. We again define the drift mode to be that described by $\Psi^r \approx \bar{\lambda}$, so that Q and the turning points z_1 are almost real. Then the quantization condition is again given by Eqs. (54)–(56), but with A_2 a function of x since $\kappa_\parallel$ now varies with x. In general this causes $h_2(x)$ in Fig. 3 to rise more steeply; hence, the factor Ψ^i in A_2 must be smaller to preserve the same radial wavenumber n as in the zero shear case. However, the point at which $\kappa_\parallel$ is chosen to vanish is arbitrary, and by moving this point to larger values of x one can restore the zero-shear value of Ψ^i. Thus for small shear the growth rate, given in certain limits by Eqs. (59) and (60), is unaffected by the shear although the radial variation of the mode is changed.

For large shear such that $\theta > 4/r_0$, the drift mode is localized by ion Landau damping. The behavior of $h_1(x)$, $h_2(x)$, and W is shown schematically in Fig. 5 for the case $x_0 = \frac{1}{2}$. The wave is localized between x_1 and x_i on either side of x_0. If the shear is so large that $\kappa_\parallel^2(x)$ varies much faster than any other factor in Q, the quantization condition (54) can be written

$$\int_{x_1}^{x_i}\left[-\frac{1}{4} + \frac{A_1 + A_3(x-x_0)^2}{2x_0} + \frac{1-m^2}{4x_0^2}\right]^{\frac{1}{2}} dx = (n+\tfrac{1}{2})\pi, \qquad (74)$$

where we have used the expansion for $\kappa_\parallel(x)$, A_1 is the same as before, and

$$A_3 = \kappa_\parallel^{*2}(x_0)e^{x_0}\Psi^i/\bar{\lambda}\epsilon_0 m\rho^4. \qquad (75)$$

For large values of n the A_3 term dominates in most of the region of integration. Equation (74) can then be integrated approximately, yielding

$$(A_3/2x_0)^{\frac{1}{2}}[(x_i - x_0)^2 - (x_1 - x_0)^2] = (2n+1)\pi. \qquad (76)$$

For simplicity we henceforth assume $\lambda = 1$; then $x_i - x_0 \approx 2m\rho^2/\kappa_\parallel^*$. With the neglect of $(x_1 - x_0)^2$, Eq. (76) yields

$$\Psi^i \approx \epsilon\kappa_\parallel^{*2}x_0(n+\tfrac{1}{2})^2\pi^2/m^3\rho^4, \quad \text{(large } n\text{)}, \qquad (77)$$

in which $\epsilon\kappa_\parallel^{*2}$ is to be evaluated at x_0. At first sight it would appear that the growth rate increases with shear, but this is true only if n is fixed. As the region of localization becomes smaller, the effective κ_r must increase to keep n constant. From the local dispersion relation, Eqs. (49)–(50), we see that Ψ^i

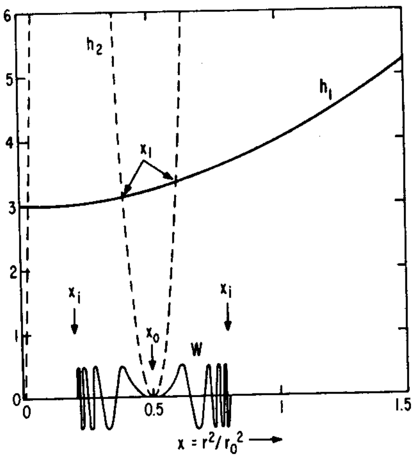

FIG. 5. Schematic of the curves h_1 and h_2, whose intersection gives the turning points x_1 for the drift mode, for the case of large shear. The perturbation is parallel to the lines of force at $x = x_0$, and ion Landau damping occurs at $x = x_i$. The behavior of the wave function W is also shown. The sign chosen for h_2 corresponds to a growing wave.

increases with κ_r; hence, it increases with $\kappa_\parallel^*$. If κ_r were kept fixed instead of n, Ψ^i would be independent of $\kappa_\parallel^*$.

To compute the experimentally interesting ratio of Ψ^i with and without shear, one must let the radial wavenumber n vary with shear in such a way as to keep the radial wavelength constant. Thus we take $n(\text{shear})/n(\text{no shear}) \approx (r_i - \bar{r})/R = 2m\rho/R\kappa_\parallel^*$. The latter equality assumes $x_0 = \frac{1}{2}$. Using Eqs. (77) and (59), we then find

$$\frac{\Omega^i\ (\text{shear})}{\Omega^i\ (\text{no shear})} = \frac{\exp(X - \frac{1}{2})}{2X} \frac{\kappa_\parallel^2}{m^2\rho^4}, \quad (\text{large } n), \quad (78)$$

where $X = R^2/r_0^2$. If L is the length of the plasma, $\kappa_\parallel$ is often given by $\kappa_\parallel = \pi a/L$. Equation (78) then becomes

$$\frac{\Omega^i\ (\text{shear})}{\Omega^i\ (\text{no shear})} = \frac{\exp(X - \frac{1}{2})}{8X} \left(\frac{\pi}{m} \frac{r_0}{a} \frac{r_0}{L}\right)^2_{\text{cm}}, \quad (79)$$

in which r_0 has been converted back to normal units. Note that this ratio is independent of the shear as long as $\theta \gg 4/r_0$, and that large values of m are preferentially stabilized by shear. For $X = O(1)$, shear diminishes the low-m growth rate significantly only if $r_0^2 \ll aL$.

For small values of n, a lower limit to Ψ^i is given by the condition $x_1 = x_i$, or $h_1(x_i) = h_2(x_i)$, where $h_1(x)$ and $h_2(x)$ are given by Eqs. (57) and (58). Since $\kappa_\parallel(x_i) = \psi = 2ma$, we obtain for large shear

$$\Psi^i \gtrsim \frac{1}{4mx_0}(x_0^2 - 2A_1x_0 + m^2 - 1)\epsilon_0 \cdot \exp(-x_0). \quad (80)$$

Comparing this with the no-shear growth rate of Eq. (60) and again setting $\kappa_\parallel = \pi a/L$, we obtain

$$\frac{\Omega^i\ (\text{shear})}{\Omega^i\ (\text{no shear})} = \frac{Xe^X h_1(x_0)}{x_0 e^{x_0} h_1(X)} \left(\frac{\pi}{4m} \frac{r_0}{a} \frac{r_0}{L}\right)^2_{\text{cm}}, \quad (\text{small } n), \quad (81)$$

which has the same general form as Eq. (79) for large n.

In the foregoing we have implicitly assumed $|x_r - x_0| > |x_i - x_0|$, where x_r is the turning point which would arise if the radial wavelength became as small as the Larmor radius, or $\kappa_r \approx \rho Q^{\frac{1}{2}} \approx 1$. Replacing Q by its dominant term, we find that we require $\Psi^i < \frac{1}{2}\epsilon_0 \exp(-x_0)/m\rho^2$. This is consistent with the growth rate of Eq. (77) if $\theta < \sqrt{2}/[\pi(n + \frac{1}{2})]$. Thus our results are valid if

$$4/r_0 \ll \theta < (\sqrt{2}/\pi)(n + \tfrac{1}{2})^{-1}.$$

This gives the maximum value of n for a given θ.

Our results on shear stabilization of the drift mode may be summarized as follows. Values of θ less than $4/r_0$ are insufficient to affect the growth rate. For $\theta \gg 4/r_0$ the growth rate for modes of the same radial wavelength λ_r is independent of shear and is given by Eq. (77) or (80). The effectiveness of shear in reducing the growth rate for different azimuthal modes goes as m^2. As shear increases, the region of localization decreases, so that large values of λ_r are eliminated; however, the short wavelength modes, which are the fastest growing, are unaffected. Absolute stability cannot be achieved until the region of localization becomes comparable to a Larmor radius. This requires $|r_i - \bar{r}| = 2ma/\kappa_\parallel' \lesssim 1$, or

$$\theta > 2\sqrt{2}. \quad (82)$$

As a numerical example we take the cesium plasma with a hard core considered previously. Using Eq. (73) with $a = 0.13$ cm, $r_0a = 1$ cm, we find that Eq. (62) requires 2.6 kA and Eq. (82) requires 14 kA in the hard core. This assumes $x_0 = \frac{1}{2}$; somewhat higher currents are required to stabilize modes localized farther from the axis.

The short-radial-wavelength modes are the most difficult to stabilize. Fortunately, these are the least effective in transporting particles across a magnetic field. The m dependence of the growth rate [see Eq. (78)] is also helpful because the fastest growing azimuthal modes are easily slowed down by shear. Therefore, a significant increase in plasma confinement time may be obtainable even if the shear is much smaller than that required for complete stability.

Discussion

The stability criterion (82) is considerably more severe than those found previously.[8,12,14] Since the completion of this work, the appearance of a paper by Krall and Rosenbluth[16] clarifying and extending the Soviet work has enabled us to understand the essential difference between our results and those of others. First, in treating the resistive, rather than the collisionless, limit we find that the explicitly imaginary term iA_2e^z in $Q(z)$[see Eq. (51)] is proportional to $k_\parallel^2$ rather than to $(k_\parallel v_e)^{-1}$, as in the case of the universal instability due to resonant electrons. Therefore, as $k_\parallel^2$ increases because of shear, the A_3 term in Eq. (74), proportional to Ψ^i, becomes dominant rather than negligible. This term allows κ_r to become arbitrarily large if Ψ^i is chosen sufficiently large, and κ_r is limited only by the breakdown of

[16] N. A. Krall and M. N. Rosenbluth, Phys. Fluids **8**, 1488 (1965).

the small-r_L expansions. Second, the localization in the absence of shear in previous papers[8,10,12,16] was attributed to a radial variation of the drift frequency Ω_{0e}. This is an artifice used to create turning points and is not intrinsic to the instability. In taking Ω_{0e} to be constant, we face up to the fact that the drift mode is basically nonlocalized. Coupled with the radial decrease of ϵ, this fact leads to our conclusion that the nature of the potential well $-\text{Re}\ Q(x)$ is not completely changed by shear, as previously thought.[8,16]

Finally, our advocacy of the stabilization criterion (82) rather than Eq. (62) stems from a difference in interpretation of the effect of the terms due to ion Landau damping. Aside from an insignificant numerical factor, our criterion of Eq. (62) is the same as that found by Krall and Rosenbluth[16] and corresponds to a shear sufficient to bring the ion Landau damping points x_i (Fig. 5) inside the plasma. Galeev[8] and Krall and Rosenbluth[16] argue that the growth rate must be averaged over the whole region of localization, and since large damping occurs near x_i, the net growth rate is negative as long as x_i lies within the plasma. Specifically, if one multiplies the equation $W'' + Q(z)W = 0$ by W^* and integrates along the real axis from $x = 0$ to $x = X$, the imaginary part gives $\int_0^X \text{Im}\ Q\ |W|^2\ dx = 0$. Since Im Q is small for the drift mode except near $x = x_i$, where the ion damping term becomes large, the integral cannot vanish unless Im Ω is such as to make Im Q small near $x = x_i$. When Im $Q(x_i)$ is written out, it is found[16] that Im Ω must be negative. We cannot find fault with this argument, but neither do we see that necessity for Im Ω to be the same everywhere. Physically, a wave packet starting near $x = x_1$ will not "know" about the existence of an ion-damping region until it has spread to $x = x_3$ and will, therefore, grow at a rate which is unaffected by ion damping. A normal mode analysis is not sufficient to describe the physical situation.

The accuracy of our results, however, can be supported by a test suggested by J. M. Dawson. The question is whether or not our treatment of x_i as a reflective turning point is valid, since the dissipative mechanism of Landau damping prevents incoming waves from x_i towards x_0. However, our analysis is valid even for running waves if the group velocity is so small that many growth times are needed for a wave packet to travel from x_0 to x_i; then the wave energy will build up before it can be dissipated. This evidently requires

$$(\partial\Psi^r/\partial\kappa_x)/\Psi^i \ll |x_0 - x_i|.$$

Equation (50) shows that the local group velocity is very small, since Ψ^r is essentially constant. To find $\partial\Psi^r/\partial\kappa_x$ one has to expand the solution of Eq. (48) to third order in g^{-1}. Using Eq. (49) for N and Eq. (50) for Ψ^i, one then finds that the small value of $\partial\Psi^r/\partial\kappa_x$ decreases even further as $x \to x_i$. Approximating $\kappa_x = Q^{\frac{1}{2}}$ by the A_3 term of Eq. (74), one can show that for $N \gg 1$, $\lambda = 1$, $x_0 = \frac{1}{2}$ the above inequality is equivalent to $\theta \ll (\epsilon r_0)^{-1}$. Since ϵr_0 is generally much less than unity, the radial group velocity is always small enough. The instability is convective, but the speed of convection is very small. Hence, Eq. (82) rather than Eq. (62) is the proper criterion for absolute stability. This point can easily be checked by experiment.

VII. EXPERIMENTAL IMPLICATIONS

Cesium Plasmas

The radial electric field in an alkali-metal plasma created by thermal ionization at hot end plates is determined by the balance of electron fluxes into and out of the end plate. If the plasma is electron rich, the flux into the plasma is $j_t \exp(e\phi/KT)$, while the flux out of the plasma is $\frac{1}{4}n\bar{v}_e$. Here j_t is the thermionically emitted flux, ϕ the plasma potential relative to the end plate, and T the common temperature of the end plate and the plasma electrons. Equating these fluxes, we find

$$e\phi/KT = \ln(\tfrac{1}{4}n\bar{v}_e/j_t). \tag{83}$$

We allow T and n, and hence $\bar{v}_e$, j_t, and ϕ, to vary with radius. With the use of Richardson's equation for j_t, differentiation of Eq. (83) gives for the radial electric field

$$E_r = -\frac{KT}{e}\frac{n'}{n} + \left(\phi_w - \phi + \frac{3}{2}\frac{KT}{e}\right)\frac{T'}{T}, \tag{84}$$

where the prime denotes $\partial/\partial r$ and ϕ_w is the work function of the end plate. In an ideal device the end plate is uniformly heated, and $T' = 0$. Then $E_r > 0$, since n' is normally negative. The radial electric field in an ideal cesium device produces an azimuthal drift equal to the ion diamagnetic drift and equal and opposite to the electron diamagnetic drift. The plasma column therefore possesses angular momentum; this is taken up by the end plates because each time an ion strikes an end plate it tends to turn the end plate in the same direction because of the ion's Larmor gyration.

If $T' \neq 0$, the electric field is as shown in Fig. 6, which is a schematic plot of Eq. (84). The stability zone, given by Eq. (33), for the $m = 2$, $n = 0$

mode of the centrifugal instability with $k_\parallel = 0$ is also shown. It is seen that the plasma is unstable to this mode if $T' = 0$ but that if T falls off with radius, as usually happens, the plasma lies in the stable zone at a not unreasonable value of T'. If T' is very large and negative, the plasma becomes unstable again. This instability may explain the oscillations observed by Buchel'nikova[17] at densities so low that finite resistivity effects could not have been important.

At high densities, electron–ion collisions allow $k_\parallel$ to be finite, and the drift mode can be excited. The allowed values of $k_\parallel$ depend on the boundary conditions imposed by the end sheaths; we have presented this computation previously.[18] Since a radial electric field is nearly always present in a cesium plasma, so that the centrifugal instability and the universal resistive overstability must be considered together, the present work is a considerable improvement over our previous treatment,[18] which was confined to the resistive drift mode and the Rayleigh–Taylor instability in plane geometry.

Stellarators

In a stellarator ions which have small velocities parallel to **B** do not greatly benefit from the rotational transform and tend to drift out of the discharge, leaving a net negative charge. The resulting E_r builds up until it gives the plasma enough rotation to stop further loss of ions. Thus a radial electric field is necessary for the operation of a stellarator, as shown recently by Bishop and Smith.[19] Fortunately, the direction of the field ($\mathcal{E}_r < 0$) is the more stable one for the centrifugal instability [Eq. (33)], and a field of the order of 50 V/cm is required to drive the $m = 2$ mode. The gravitational instability due to curvature of the magnetic field dominates over the centrifugal instability for $|E_r| < 100$ V/cm. In any case, these instabilities with $k_\parallel \approx 0$ are easily stabilized by shear, as shown by Eq. (71).

The resistive drift modes with finite $k_\parallel$ are far more dangerous. The criterion of Eq. (62) is barely achievable in a stellarator, and this is sufficient to slow down only the large-m modes. The criterion of Eq. (82) for complete stability is unattainable. Thus there is no solace to be had from the linear theory, but one can hope that a nonlinear theory will show that the large-κ_r modes do not affect the plasma confinement. Another possibility is to allow the interior of the plasma to be unstable, so that the density gradient is small there, and to try to shear-stabilize the boundary layer, in which the density and potential gradients are concentrated. This layer would be of the order of several Larmor radii thick, and obviously the stability of this layer would be very difficult to analyze.

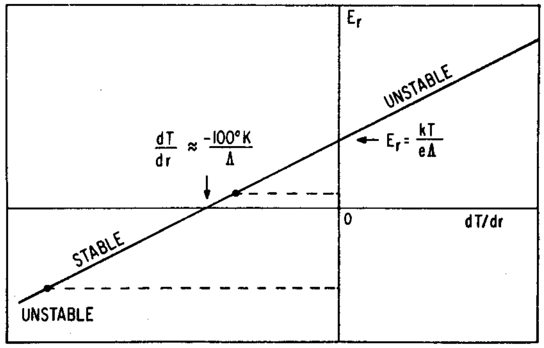

Fig. 6. The radial electric field in a cesium plasma as a function of the temperature gradient in the emitting end plate. The stability zone is for the $m = 2$ mode of the centrifugal instability with $k_\parallel = 0$. Here Λ is the scale length of the density gradient.

Rotating Plasmas

In devices such as Ixion,[20] a large radial electric field is used to ionize and help confine a plasma. Such rotating plasmas have been reviewed by Lehnert.[21] Taking Ixion as a typical example, we find that $\Omega_0 \approx 0.05$ so that the gyration radii are still much smaller than the plasma radius, and our theory is valid. The plasma was found to be "stable" for $s < 10^2$. According to Eq. (32) the plasma should be well outside the limits for stability against the $k_\parallel = 0$ mode. If the end plates were conducting, the $k_\parallel = 0$ mode would be absent, but the drift mode should occur. The length of the plasma and the requirement of no Landau damping would limit the unstable modes to those with $m \gg 20$. Such high-frequency modes could well have escaped detection. The current measuring loop used to check the insulating properties of the end plate could not, of course, show whether or not the end plate was a short circuit for high-m modes.

Another instability apparently develops for $s > 10^2$, so that the rotation velocity cannot be raised above this limit. We are unable to explain this. Of course, the theory is not valid for such large values of

[17] N. S. Buchel'nikova, Nucl. Fusion **4**, 165 (1964).
[18] F. F. Chen, J. Nucl. Energy **C7**, 399 (1965).
[19] A. S. Bishop and C. Smith, Princeton Plasma Physics Laboratory Report MATT–Q–22 (1964), p. 278.
[20] D. A. Baker, J. E. Hammel, and F. L. Ribe, Phys. Fluids **4**, 1534, 1549 (1961).
[21] B. Lehnert, in *Plasma Physics and Thermonuclear Research*, edited by C. L. Longmire, J. L. Tuck, and W. B. Thompson (The Macmillan Company, New York, 1963), Vol. 2, p. 201.

s; and it is possible that if one were to do the theory for large s, one could explain the velocity limit without invoking the presence of neutral atoms.

Beam-Plasma Discharges

When an energetic electron beam shot into a neutral gas is used to create a plasma, low-frequency oscillations are often observed in addition to the expected high frequency phenomena due to beam-plasma interactions. We have recently shown[22] that the low-frequency oscillations cannot be drift waves directly excited by the beam. However, they may well be caused by the centrifugal instability discussed in this paper because a large radial electric field can be built up by the injection of fast electrons.

VIII. ACKNOWLEDGMENTS

We have benefited from several helpful discussions with E. A. Frieman, J. M. Greene, and R. M. Kulsrud. L. Goldberg of the Plasma Physics Laboratory Computing Group performed the numerical calculations.

Use was made of computer facilities supported in part by National Science Foundation Grant NSF-GP579. This work was performed under the auspices of the United States Atomic Energy Commission, Contract No. AT(30-1)-1238.

APPENDIX I. THE VISCOSITY TENSOR IN CYLINDRICAL COORDINATES

The nondimensional ion viscosity tensor in strong magnetic fields such that $\alpha^2 \gg 1$ is given in Ref. 4 in Cartesian coordinates,

$$\begin{aligned}
-\Pi_{xx} &= \alpha(\Upsilon_{xx} + \Upsilon_{yy}) + \Upsilon_{xy}, \\
-\Pi_{yy} &= \alpha(\Upsilon_{xx} + \Upsilon_{yy}) - \Upsilon_{xy}, \\
-\Pi_{zz} &= 2\alpha\Upsilon_{zz}, \\
-\Pi_{xy} &= -\Pi_{yx} = \frac{1}{2}\left(\Upsilon_{yy} - \Upsilon_{xx} + \frac{1}{\alpha}\Upsilon_{xy}\right), \\
-\Pi_{xz} &= -\Pi_{zx} = 2\left(\Upsilon_{yz} + \frac{1}{\alpha}\Upsilon_{xz}\right), \\
-\Pi_{yz} &= -\Pi_{zy} = 2\left(\frac{1}{\alpha}\Upsilon_{yz} - \Upsilon_{xz}\right),
\end{aligned} \tag{I-1}$$

where $\alpha = \omega_c \tau_{ii}$,

$$\Upsilon = \tfrac{1}{2}(\nabla v + \nabla v^T) - \tfrac{1}{3}(\nabla \cdot v)\mathbf{I}, \tag{I-2}$$

$$\tau_{ii} = \frac{5}{8\pi^{\frac{1}{2}}} \frac{m_i^{\frac{1}{2}}(KT_i)^{\frac{3}{2}}}{ne^4 \ln \Lambda}. \tag{I-3}$$

To transform to cylindrical coordinates, we replace x and y by r and θ, respectively, in Eq. (I-1) and evaluate Υ by writing out $\nabla = (\hat{\mathbf{r}}\partial/\partial r) + [(\hat{\boldsymbol{\theta}}/r)\partial/\partial\theta] + (\hat{\mathbf{z}}\partial/\partial z)$ and $v = \hat{\mathbf{r}}v_r + \hat{\boldsymbol{\theta}}v_\theta + \hat{\mathbf{z}}v_z$ and performing the operations indicated in Eq. (I-2), taking care to differentiate the unit vectors: $\partial\hat{\mathbf{r}}/\partial\theta = \hat{\boldsymbol{\theta}}$, $\partial\hat{\boldsymbol{\theta}}/\partial\theta = -\hat{\mathbf{r}}$. For the relevant components of $\mathbf{\Pi}$ we then obtain Eq. (4).

To evaluate $\mathbf{P} \equiv -(\nabla\cdot\mathbf{\Pi} + \mathbf{\Pi}\cdot\delta\hat{\mathbf{r}})_1$, we write $\mathbf{\Pi}$ as $(\hat{r}\Pi_{rr}\hat{r} + \hat{\theta}\Pi_{\theta\theta}\hat{\theta} + \cdots$ etc.), operate on it with ∇, again taking care to differentiate the unit vectors, and *then* form the scalar product. We then obtain

$$\begin{aligned}
-P_r &= \Pi_{rr,r} + \frac{1}{r}\Pi_{\theta r,\theta} + \Pi_{zr,z} \\
&\qquad + \frac{1}{r}(\Pi_{rr} - \Pi_{\theta\theta}) + \delta\Pi_{rr}, \\
-P_\theta &= \Pi_{r\theta,r} + \frac{1}{r}\Pi_{\theta\theta,\theta} + \Pi_{z\theta,z} \\
&\qquad + \frac{1}{r}(\Pi_{r\theta} + \Pi_{\theta r}) + \delta\,\Pi_{\theta r}, \\
-P_z &= \Pi_{rz,r} + \frac{1}{r}\Pi_{\theta z,\theta} + \Pi_{zz,z} \\
&\qquad + \frac{1}{r}\Pi_{rz} + \delta\Pi_{zr}.
\end{aligned} \tag{I-4}$$

Here $\mathbf{\Pi}$ is the first-order $\mathbf{\Pi}$ and will contain terms like $\alpha_1\Upsilon_0$ as well as $\alpha_0\Upsilon_1$, since α is a function of $n = n_0 + n_1$. However, the former terms may be neglected because Υ_0 is very small if Ω_0 is uniform. Thus we may substitute α_0 for α. In taking the derivatives indicated in Eq. (I-4), we use the relation $\alpha' \approx -\delta\alpha$, obtained from Eq. (I-3).

We next neglect the Π_{zr} and $\Pi_{z\theta}$ components in Eq. (I-4), whereupon the transverse and z components of $\mathbf{P}$ separate. Substituting Eq. (4) into Eq. (I-4) and performing the differentiations, we obtain for the transverse components

$$P_r = A_{rr}v_r + A_{r\theta}v_\theta, \quad P_\theta = A_{\theta r}v_r + A_{\theta\theta}v_\theta, \tag{I-5}$$

where

$$\begin{aligned}
A_{rr} &= -\frac{\alpha}{3r}\left[\frac{1}{r} - \frac{\partial}{\partial r}\left(r\frac{\partial}{\partial r}\right)\right] \\
&\qquad + i\gamma\left(\frac{\delta}{2} + \frac{1}{r}\right) - \gamma^2/4\alpha, \\
A_{\theta\theta} &= -\frac{1}{4\alpha r}\left[\frac{1}{r} - \frac{\partial}{\partial r}\left(r\frac{\partial}{\partial r}\right)\right] + i\gamma\left(\frac{\delta}{2} + \frac{1}{r}\right) \\
&\qquad - \alpha\gamma^2/3 - \frac{\delta}{2\alpha}\left(\frac{1}{r} - \frac{\partial}{\partial r}\right),
\end{aligned} \tag{I-6}$$

[22] F. F. Chen, Phys. Fluids 8, 2115 (1965).

$$A_{r\theta} = -\frac{1}{2}\left(\gamma^2 - \frac{\partial^2}{\partial r^2}\right) + \left[\frac{1}{2}\left(\delta + \frac{1}{r}\right) + i\gamma\left(\frac{\alpha}{3} + \frac{1}{4\alpha}\right)\right]\frac{\partial}{\partial r} - \frac{1}{r}\left[\frac{1}{2}\left(\delta + \frac{1}{r}\right) + i\gamma\left(\frac{\alpha}{3} + \frac{1}{4\alpha}\right)\right],$$

$$A_{\theta r} = \frac{1}{2}\left(\gamma^2 - \frac{\partial^2}{\partial r^2}\right) - \left[\frac{1}{2}\left(\delta + \frac{1}{r}\right) - i\gamma\left(\frac{\alpha}{3} + \frac{1}{4\alpha}\right)\right]\frac{\partial}{\partial r} + \frac{1}{r}\left[\frac{1}{2}\left(\delta + \frac{1}{r}\right) + i\gamma\left(\frac{\alpha}{3} + \frac{1}{4\alpha}\right) + \frac{i\delta\gamma}{2\alpha}\right].$$

Here we have neglected v_z and have used $\partial/\partial\theta = im/r \equiv i\gamma$. The collisionless limit cannot be obtained by letting $\alpha \to \infty$ because of the presence of terms proportional to α. However, as shown in Ref. 4, these terms enter in such a way as to cancel themselves, so that the collisionless limit is correctly obtained by simply omitting the terms in which α appears. We then obtain Eq. (12).

APPENDIX II. FINITE DEBYE LENGTH

To take finite Debye length effects into account we define $\nu_i = n_{i1}/n_{i0}$, $\nu_e = n_{e1}/n_{e0}$, $n_{i0}/n_{e0} = s_0$, $\sigma = h^2/a^2$, where h is the Debye length $(KT_e/4\pi n_{e0}e^2)^{\frac{1}{2}}$. Poisson's equation in first order then reads

$$\sigma[r^{-1}(r\chi')' - \gamma^2\chi - \kappa_\parallel^2\chi] = \nu_e - s_0\nu_i \approx -\sigma\gamma^2\chi, \quad \text{(II-1)}$$

where we have assumed $\kappa_\parallel = 0$ and $n \ll m$. Equations (15)–(19) for the ions are still valid if ν is replaced by ν_i. Equation (9) for the electrons is still valid if ν is replaced by ν_e. Equations (9), (19), and (II-1) are now three equations for ν_e, ν_i, and χ. Replacing χ by the variable $\Phi \equiv \chi + \lambda\nu_i$, we can obtain the differential equation (25) for Φ, except that N now contains terms involving s_0 and σ. The latter are related by the zero-order Poisson equation, which yields

$$s_0 = 1 + \sigma\nabla\cdot\mathcal{E}_0 \approx 1 - 2\sigma(2\lambda r_0^{-2} + \Omega_0), \quad \text{(II-2)}$$

with the help of Eqs. (7) and (8). After performing the indicated algebra and transforming to Whittaker's equation as before, we obtain Eq. (41), with $N(z)$ now a function of z only through terms containing σ. If σ is small, we can estimate its effect by neglecting the z dependence of N and setting $N = 2n + m$, as before. We then obtain, for $\psi = O(\rho^2)$, the dispersion relation

$$(N + \tfrac{1}{2}\sigma\gamma^2r_0^2)\psi^2 + 2m\left[\lambda\left(\frac{1-N}{r_0^2} - \frac{\sigma}{2}\right) + \Omega_0\right]\psi + m^2\left[\Omega_0^2 + \frac{2\sigma\lambda}{r_0^2}(\lambda\gamma^2 - 4\lambda r_0^{-2} - 2\Omega_0)\right] = 0, \quad \text{(II-3)}$$

which reduces to Eq. (31) when $\sigma = 0$ and $\lambda = 1$. It is clear that the σ term in the coefficient of ψ adds to the finite-r_L stabilization. The σ term in the last bracket can possibly be destabilizing, but if $\Omega_0 = O(\rho^2)$ and $\sigma = O(\rho^2)$ this term is negligible. Also, when $\lambda \to \infty$ the equation gives stability. Thus finite Debye length gives a stabilizing effect.